Journal of Applied Polymer Science

Fiber preparation and mechanical properties of recycled polypropylene for reinforcing concrete

Shi Yin,[1] Rabin Tuladhar,[1] Robert A. Shanks,[3] Tony Collister,[2] Mark Combe,[2] Mohan Jacob,[1] Ming Tian,[4] Nagaratnam Sivakugan[1]

[1]School of Engineering and Physical Sciences, James Cook University, Queensland 4811, Australia
[2]Fibercon, Queensland 4051, Australia
[3]School of Applied Sciences, RMIT University, Melbourne, Victoria 3001, Australia
[4]Key Laboratory of Carbon Fiber and Functional Polymers, Ministry of Education, Beijing University of Chemical Technology, Beijing 100029, China
Correspondence to: R. Tuladhar (E-mail: rabin.tuladhar@jcu.edu.au)

ABSTRACT: Polypropylene (PP) fibers have been widely used to reinforce concrete footpaths as an alternative to steel mesh. The reinforcing effect of the PP fiber is directly proportional to its tensile strength and Young modulus. This research explored the feasibility of using an improved melt spinning and hot drawing process to produce virgin and recycled PP fibers of high mechanical properties in an industrial scale. Commercial grade granules of virgin PP, recycled PP and HPDE were mixed in different proportions in preparing five different types of fibers. All the fibers obtained high tensile strength and Young modulus. A relationship between the structural parameters and mechanical properties was then established. It was observed that the melt spinning and hot drawing process formed both α-form and β-form crystals in the PP fibers, and significantly improved crystallinity from about 50% to 80%. © 2015 Wiley Periodicals, Inc. J. Appl. Polym. Sci. **2015**, *132*, 41866.

KEYWORDS: crystallization; differential scanning calorimetry; manufacturing; mechanical properties; recycled PP fiber

Received 4 October 2014; accepted 11 December 2014
DOI: 10.1002/app.41866

INTRODUCTION

Concrete is widely used in construction industry because all the raw materials required are widely available and are of low cost. Concrete is very strong in compression; however, it has a very low tensile strength. To improve its tensile strength, reinforcing steel is often used in concrete. Apart from traditional steel reinforcement, various fibers are used to improve the properties of concrete, such as steel fiber, glass fiber, natural fiber, and synthetic fiber.[1]

The fibers in concrete can bridge concrete cracks to reduces stress intensity factor at the crack tip and thus to prevents the propagation of the crack tip.[2] In addtion, the fiber bridging can decrease crack width, which prevents water and contaminants from entering the concrete matrix to corrode reinforcing steel and degrade concrete.[3] The fibers can effectively control and arrest crack growth, hence preventing plastic and dry shrinkage cracks,[4] retaining integrity of concrete,[5] and altering the intrinsically brittle concrete matrix into a tougher material with enhanced crack resistance and ductility.[6] The reinforcing effect of fiber is directly proportional to its tensile strength and Young modulus.[7]

Several techniques and methods have been developed to produce thermoplastic fibers with high tensile strength and Young modulus.[7–13] The melt spinning and hot drawing technique is a common method of producing thermoplastic fibers for toughening concrete. The fibers are firstly extruded, and then slowly stretched in an oven with a temperature of 130–150°C.[10] This method can give polypropylene (PP) fibers of 250–650 MPa tensile strength and Young modulus of 5–15 GPa.[11] Another popular processing technique is extruding poly(ethylene terephthalate) (PET), PP or polyethylene (PE) pellets through a rectangular die to form film sheets. The resulting film sheets are then slit longitudinally into equal width tapes.[12] Kim *et al.*[13] melted PET bottles, and then pressed and rolled them into a roll-type sheet (0.2–0.5 mm in thick). The sheets were slit into 1–1.3 mm width thin strands by a slitting machine. Finally, the fibers obtained a tensile strength of 420.7 MPa, and elastic modulus of 10.2 GPa.

A common deficiency of these methods is that they are based on laboratory processes, and they have an extremely low production rate and ensuing high cost. Our research, on the other hand, is focused on development of an improved melt spinning

Table I. Characteristics of Raw Materials of Plastic Fibers

Raw material	Virgin PP granule	Recycled PP granule	HDPE granule
Density (g/cm^3)	0.90	0.90–0.92	0.957
Melt flow rate (MFI, 2.16 kg, dg/min)	3.5 (at 230°C)	13 (at 230°C)	0.4 (at 190°C)
Tensile stress at yield (MPa)	31	35	31.4
Flexural modulus (GPa)	1.25	1.48	
Notched izod impact strength (23°C, type 1, Notch A, kJ/m^2)	4.7	3.5	5.8

and hot drawing process under industrially feasible conditions. To reduce landfill of plastic wastes and improve environmental sustainability, recycled PET fibers have been recently become a focus of research.[7,10,12–15] However, recycled PP fiber literature is very limited. This article investigates the possibility of producing recycled PP fiber with high mechanical properties by this process. High-density polyethylene (HDPE) and virgin PP were mixed into the fiber from recycled PP to improve mechanical properties as well. Finally, a more detailed investigation of the structure and relationship between the structural parameters and mechanical properties is presented in this study.

Similar with other polymer fibers, the tensile strength and Young modulus of PP fibers are affected by their physical structure, which is normally controlled by both the choice of starting material and the fiber formation conditions.[16–18] The various conditions for fiber formation during melt spinning and hot drawing caused different arrangement of the supermolecular structural elements, further leading to different fiber mechanical properties. The starting material with different molecular structure, such as different polymer molar mass and molar mass distribution, contributes to determination of the final mechanical properties of PP fibers.[19] Structural changes in terms of the crystallinity and crystal size distribution, orientation of the amorphous and crystalline phases, and the deformation behavior at the crystal lattice and lamellae scales occurring in the semicrystalline PPs due to the hot drawing process have been extensively studied.

Lupke *et al.*[20] found that the hot drawing process transformed the initially spherulitic morphology of the PP film into a stacked lamellae morphology (shish kebab) by partial melting. Tabatabaei *et al.*[21] found that the deformation behavior of the crystal structure was dependent on the draw ratio. With increase of drawing rate, the crystal lamellae were first sheared and oriented along the drawing direction and then, at high drawing rate, they were deformed and created a fibrillar structure. Feng *et al.*[22] reported that during the hot stretching process, the chain disentanglement process dominates, resulting in the relaxation of restrained tie chains and the formation of more folded-chain lamellae. Choi and White[23] found that the mesomorphic structure of isotactic PP (iPP) is more readily formed in lower tacticity fibers, and significant amounts of hexagonal β-form crystals are found in low tacticity iPP fibers spun at high draw-down ratios. Low tacticity iPP fibers exhibited a significant decrease in the crystalline chain-axis orientation at high draw-down ratios, resulting from increased epitaxially branched lamellae. Diana[24] found that in the hot drawing process, the initial metastable structure of low crystallinity was disrupted and a chain-axis orientation of monoclinic crystalline modification was developed. The hot drawing process increased the crystallite size and crystallinity, the orientation of crystalline domains, and average orientation of the macromolecular chains and resulted in extensive fibrillation and void formation.[24]

This research has explored the industrial feasibility of using melt spinning and hot drawing process to produce PP fiber under factory conditions instead of laboratory conditions. Virgin PP fiber of high tensile strength and Young modulus has been successfully produced by this method. A relationship has been established between mechanical properties, crystallinity, crystal structure and orientation of PP in the fiber. However, the production of recycled plastics with sufficient mechanical properties is still a major challenge due to degradation during their service life and heat processing stage. The aim of this research is to improve the tensile strength and Young modulus of fibers from recycled PP produced through the melt spinning and hot drawing process. Besides 100% recycled PP fiber, 50% of virgin PP and 5% of HDPE were mixed into the recycled PP fiber to produce 50 : 50 Virgin-Recycled PP fiber and 5 : 95 HDPE-Recycled PP fiber, respectively. The mechanical properties of these recycled fibers produced by the melt spinning and hot drawing process are presented and compared with the virgin PP fiber. The effects of 50% of virgin PP and 5% of HDPE on fiber from recycled PP are studied in terms of crystal structure and crystallinity by differential scanning calorimetry (DSC) and wide-angle X-ray scattering (WAXS).

EXPERIMENTAL

Materials

Raw materials for producing virgin PP, recycled PP, and HDPE used in this study are commercial grade granules. Their characteristics given in the manufacturer specifications are presented in Table I.[25–27] Five types of fibers were prepared: (a) 100% virgin PP fiber, (b) 5 : 95 HDPE-virgin PP fiber containing 5% HDPE and 95% virgin PP, (c) 100% recycled PP fiber, (d) 5 : 95 HDPE-recycled PP fiber produced by extruding 5% HDPE with 95% recycled PP, and (e) 50 : 50 virgin-recycle fiber that was made by extruding mixed raw materials of 50% virgin PP and 50% recycled PP.

Preparation of the Thermoplastic Fibers

As shown in Figure 1, the plastic granules were fed into a single-screw extruder and melted. Temperatures of five heating zones of the extruder were set at 218, 223, 225, 233, and 235°C. Fibers were then extruded into a water bath from the nozzle at the tip of the extruder. The extruded fiber was pulled to a chill roll and hot-drawn in the oven at 120–150°C. The resulting

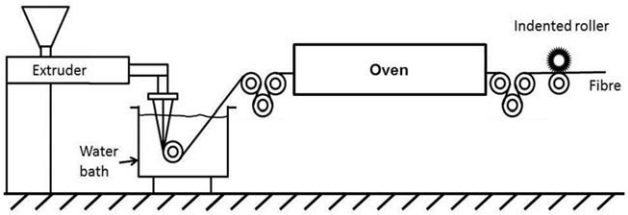

Figure 1. Extrusion apparatus for monofilaments.

fibers through the second chill roll were smooth and had a circular cross-section of around 0.9 mm^2. An indented roller die was used to mark indents on the fibers, in order to increase the bond strength between the fibers and concrete. After indentation, fibers were cut into a length of 47 mm as Figure 2.

Measurements

Tests for tensile strength and Young modulus were performed on the virgin and recycled PP fibers according to ASTM D3822-07.[28] The tensile test instrument used for the tests was United STM "Smart" Test System (STM-50KN) from United Calibration Corporation and was equipped with a 2 kN load cell and data acquisition software. Distance between the clamps was adjusted to obtain a gauge length of 25.4 mm, and extension speed was set as 60% of the gauge length/min (15.24 mm/min). 30 specimens were tested for each sample. Testing temperature was 20 ±2°C.

Fourier transform infrared (FTIR) measurements were carried out with a Perkin-Elmer spectrum 100 FTIR Spectrometer. Fiber orientation degree was obtained by measuring the FTIR spectra with radiation parallel and perpendicular to fiber direction. Contents of crystal and amorphous were calculated in terms of intensity of the absorption bands at 998 and 1153 cm^{-1} bands, respectively.[29]

Non-isothermal crystallization and melting behavior of the fibers were studied using a Perkin-Elmer Pyris-1 differential scanning calorimeter (DSC). About 3 mg of the PP was weighed accurately and encapsulated in an aluminium pan. Samples

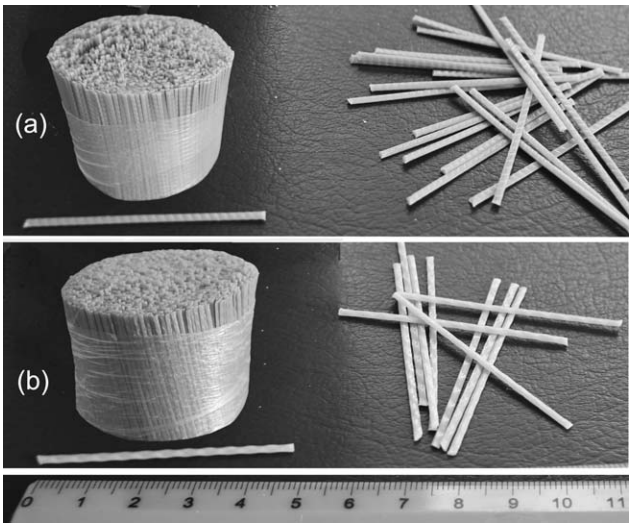

Figure 2. Virgin (a) and recycled (b) PP fibers.

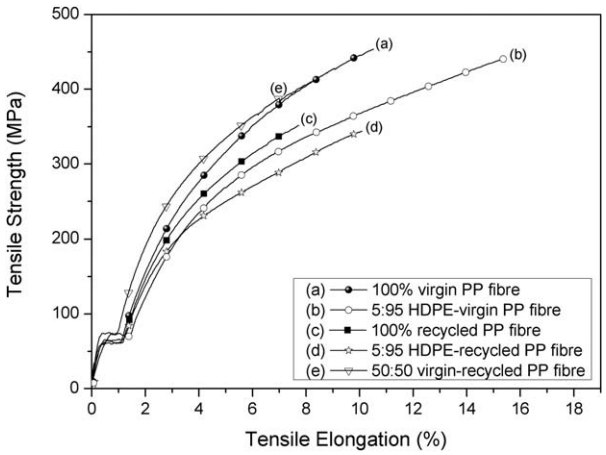

Figure 3. Typical stress–strain curves of the PP fibers.

were heated from 30°C to 220°C at the heating rate of 10 K/min to study the melting behavior of the fibers. The crystallinity and crystalline structure of the PP fibers can be calculated through this heating. The samples were then kept at 220°C for 5 min to eliminate their thermal history. Subsequently, the samples were cooled to 30°C at the rate of 10 K/min to study their crystallization behavior with temperature; and reheated to 220°C at the heating rate of 10 K/min to study their melting behavior with temperature. All measurements were carried out under a nitrogen atmosphere to avoid thermal-oxidative degradation. In both crystallization and melting experiments, the peak temperatures were obtained for crystallization temperature (T_c) and melting temperature (T_m), respectively. The crystallinity of the PPs was calculated using eq. (1)[30]

$$\text{Crystallinity} = \frac{\Delta H_f}{\Delta H_f^0} \times 100 \quad (1)$$

where ΔH_f is the heat of fusion of PP fibers and ΔH_f^0 is the heat of fusion of a totally crystalline PP taken as 207 J/g.[31]

WAXS measurements were performed in reflection mode at ambient temperature using an X-ray diffractometer (Bruker D4 Endeavor). The generator was set at 40 kV and 40 mA and the copper Cu-Kα radiation was selected using a graphite crystal monochromator.

RESULTS AND DISCUSSION

Mechanical Properties

As can be seen in Figure 3, all the fibers produced by the melt spinning and hot drawing process show a brittle mode of failure, with a short elastic period of steep slope and a regime of sharply rising specific stress until fracturing occurred at strains between 8 and 16%. Table II presents average of the tensile strength, Young modulus and elongation of these fibers and their standard deviation. Compared with the mechanical properties of virgin and recycled PP raw materials in Table I, the melt spinning and hot drawing process offers the PP fibers much higher mechanical properties. The virgin PP fiber obtains highest tensile strength at 457.1 MPa and very high Young modulus at 7526 MPa, while the recycled PP fiber exhibits 341.6 MPa of tensile strength and comparable Young modulus (7115 MPa).

Table II. Tensile Properties of the PP Fibers

PP compositions	Tensile strength (MPa)		Young modulus (MPa)		Tensile elongation (%)	
	Mean	Standard deviation	Mean	Standard deviation	Mean	Standard deviation
100% virgin PP fiber	457.1	31.7	7526	2011	10.6	1.4
5 : 95 HDPE-virgin PP fiber	436.0	23.2	6837	1538	16.5	2
100% recycled PP fiber	341.6	29.3	7115	2083	8.4	2.2
5 : 95 HDPE-recycled PP fiber	341.9	27.6	6467	2326	9.4	1.7
50 : 50 virgin-recycled PP fiber	435.5	26.5	9016	1919	8.1	1.4

As the raw material properties in Table I, the MFI of raw recycled PP is 13 dg/min, which is much higher than that of raw virgin PP (only 3.5 dg/min). This means that the fiber from recycled PP has much lower molar mass and hence shorter molecular chains than the virgin PP fiber.[32] During the service life of PP products, the recycled PP materials normally have natural aging from long exposure to the air, light, moisture, temperature and weathering.[33] Moreover, the multiple processes under high shear forces and temperatures, and the presence of impurities and oxygen severely damage molecular chain of PPs, including crosslinking, chain scission and formation of double bonds.[34] The chain scissions and degradation make the molecular chain easier to be pulled out, forming disentanglement and promoting nucleation of micro-voids and micro-cracks.[35] Therefore, the recycled PP fiber had much lower tensile strength and elongation at break than the virgin PP fiber.

When 5% HDPE was mixed with both the recycled and virgin PP fibers, the Young modulus of both fibers were decreased and the tensile elongations were increased compared with the 100% recycled and virgin PP fibers. This indicated that the HDPE brought ductility to the PP fibers. However, when 50% of the virgin PP was mixed with 50% of the recycled PP, the Young modulus was considerably increased to 9016 MPa, which was even higher than that of virgin PP fiber, and the tensile strength remained as high as the virgin PP fiber at 435.5 MPa. Therefore, the recycled PP fiber can obtain good ductility from the 5% of HDPE and can be well modified to obtain high tensile strength and Young modulus by mixing with 50% of virgin PP.

Molecular Orientation by FTIR

Molecular orientation of the recycled PP fiber and its raw material was measured by using FTIR spectra with radiation parallel and perpendicular to the fiber and raw material. The intensity of absorption brands at 998 and 1153 cm^{-1} were used to calculate the contents of crystal and amorphous, respectively.[29] For quantitative estimation of orientations, the dichroic ratios of 998 and 1153 m^{-1} bands, R_{998} and R_{1153}, were calculated with dividing the intensity of absorption brands in parallel direction ($A_{parallel}$) by the intensity in perpendicular direction ($A_{perpendicular}$), that is, $R = A_{parallel}/A_{perpendicular}$. The degree of orientation f of crystal and amorphous was further calculated through eq. (2)[36]

$$f=(R-1)/(R+2) \quad (2)$$

As shown in eq. (2), the closer to zero the absolute value of f is, the less orientation the molecules have, and vice versa. As can be seen in Figure 4(a), the recycled raw material in both parallel and perpendicular directions shows similar intensity of absorption brands at 998 and 1153 cm^{-1}. The f_{998} and f_{1153} were calculated as −0.09 and 0.05, respectively. Therefore, the raw material has not obvious molecular orientation. However, after the melt spinning and hot drawing process, the intensities of absorption brands at 998 cm^{-1} of the recycled PP fiber exhibit significant difference on the both directions as Figure 4(b). The f_{998} was calculated as −0.5, thus the crystal phase of the recycled PP fiber exhibits considerable molecular orientation.

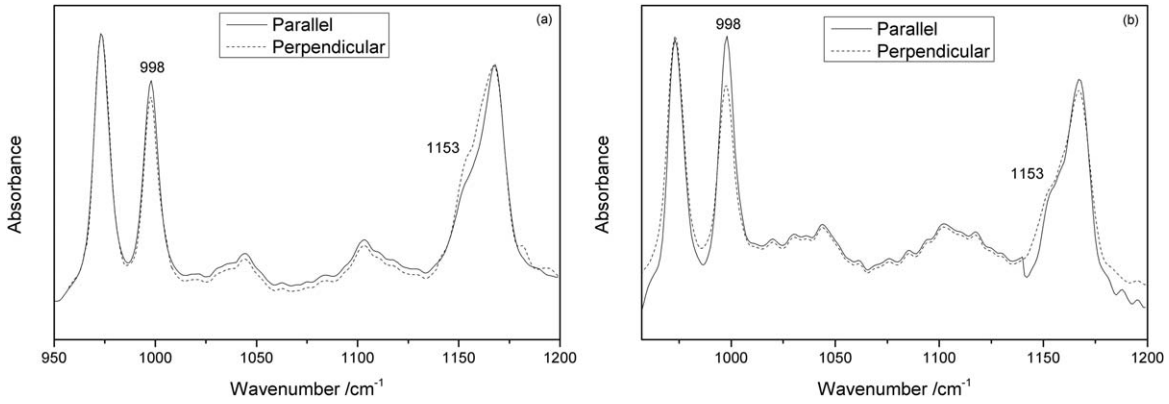

Figure 4. FTIR spectra of recycled raw material (a) and recycled PP fiber (b) on parallel and perpendicular directions to the raw material and the fiber.

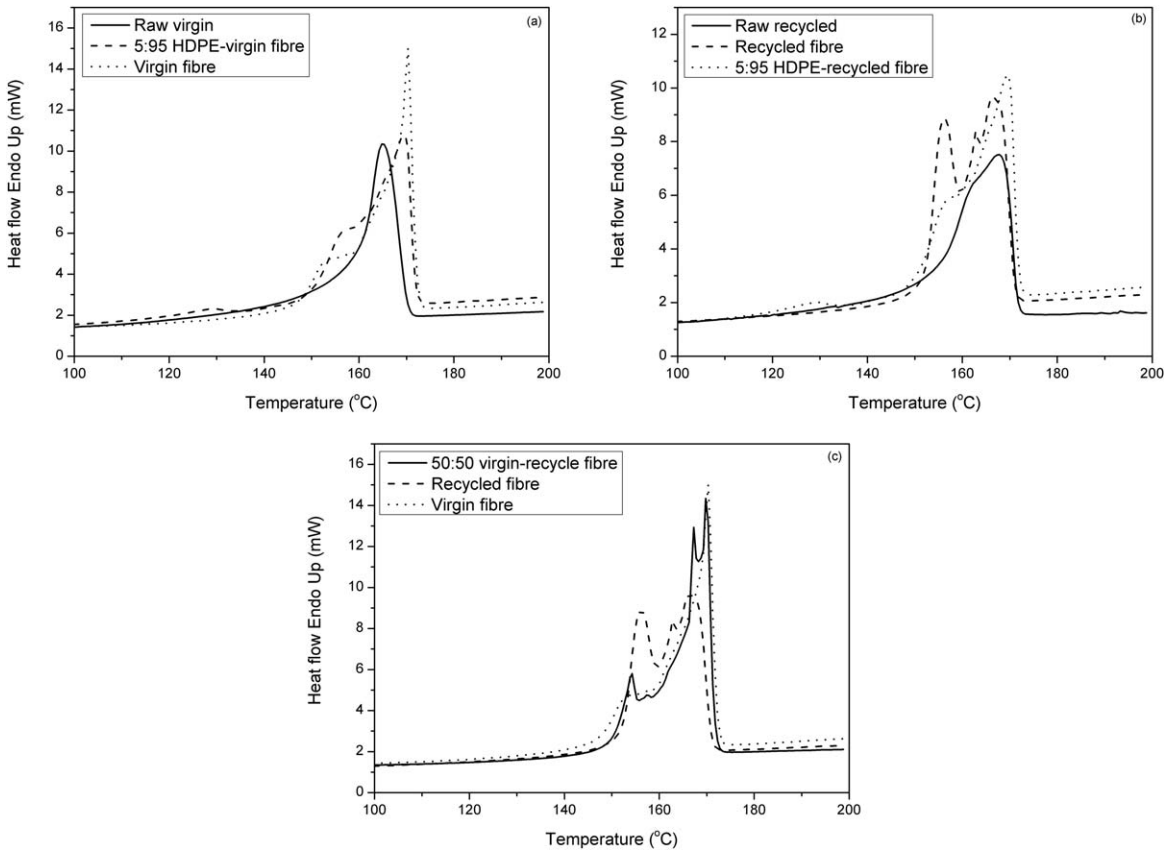

Figure 5. DSC heating curves of the PP fibers and their raw materials (First round of heating from 30 to 220°C).

Crystal Structure and Crystallinity by DSC

The crystal structure of the PP fibers was studied by DSC. As shown in Figure 5(a,b), the raw material of recycled PP has a broader melting endotherm than that of the virgin PP, which indicates that the raw recycled PP has more crystals of different sizes, and the raw virgin PP has more uniform crystal sizes. From the Table III the raw recycled PP exhibits higher heat of fusion (ΔH) than the raw virgin PP, indicating the raw recycled PP has higher crystallinity. This is why the raw recycled PP has higher mechanical properties than the raw virgin PP as Table I. As Table I, the raw recycled PP has much higher MFI than the raw virgin PP, indicating that the raw recycled PP has lower molar mass and shorter molecular chains. In the processing stage and service life of the recycled PP, chain scissions frequently occur, thus significantly reducing the molar mass and shortening the molecular chains. The lower molar mass and shorter molecular chains are easier to rearrange, orient and form into crystals than the longer molecular chains of the raw virgin PP.[37]

As shown in Table III, the ΔH and crystallinity of the raw virgin PP are very small (only 76.2 J/g and 36.8%, respectively). However, after the melt spinning and hot drawing process, the ΔH and crystallinity of the virgin PP fiber are increased dramatically to 106.7 J/g and 51.5%, respectively. Similar with the recycled PP, the process improved the crystallinity of the recycled PP from 41.5% to 50.9%. Furthermore, as Figure 5(c) the virgin and recycled PP fibers exhibit a double-melting endotherm at around 154 and 168°C. The peak located at 154°C is ascribed to the β-form crystals and the other is to the α-form crystals.[21] According to Huo *et al.*, this oriented molecular chains formed α row-nuclei and the oriented α row-nuclei can induce to form β-crystals.[38] Somani *et al.*[39] reported that the PP fibers which have a double-melting endotherm show a specific shish-kebab structure. The shish in PP had a melting temperature of about 5–10°C higher than that of the kebabs and about 15–20°C higher than that for spherulites.

On the α-form crystallization in Table III, the virgin PP fiber exhibited higher peak melting temperature (T_m) than its raw material. As Zhao and Ye,[40] the high-temperature endotherm represents the melting of the highly chain-extended and the highly oriented crystalline blocks formed during the hot drawing process and the low-temperature endotherm is due to the melting of strained non-crystalline region and some partially oriented lamellar. According to Elias *et al.*,[41] the hot drawing process also can result in a connectivity of molecular chains in the shish or fibrils, thus increasing the crystal thickness. Therefore, a higher melting point was obtained by the virgin PP fiber. However, the recycled PP fiber had slightly lower peak temperature of melting than its raw material probably because of molecular defects and lower purity.

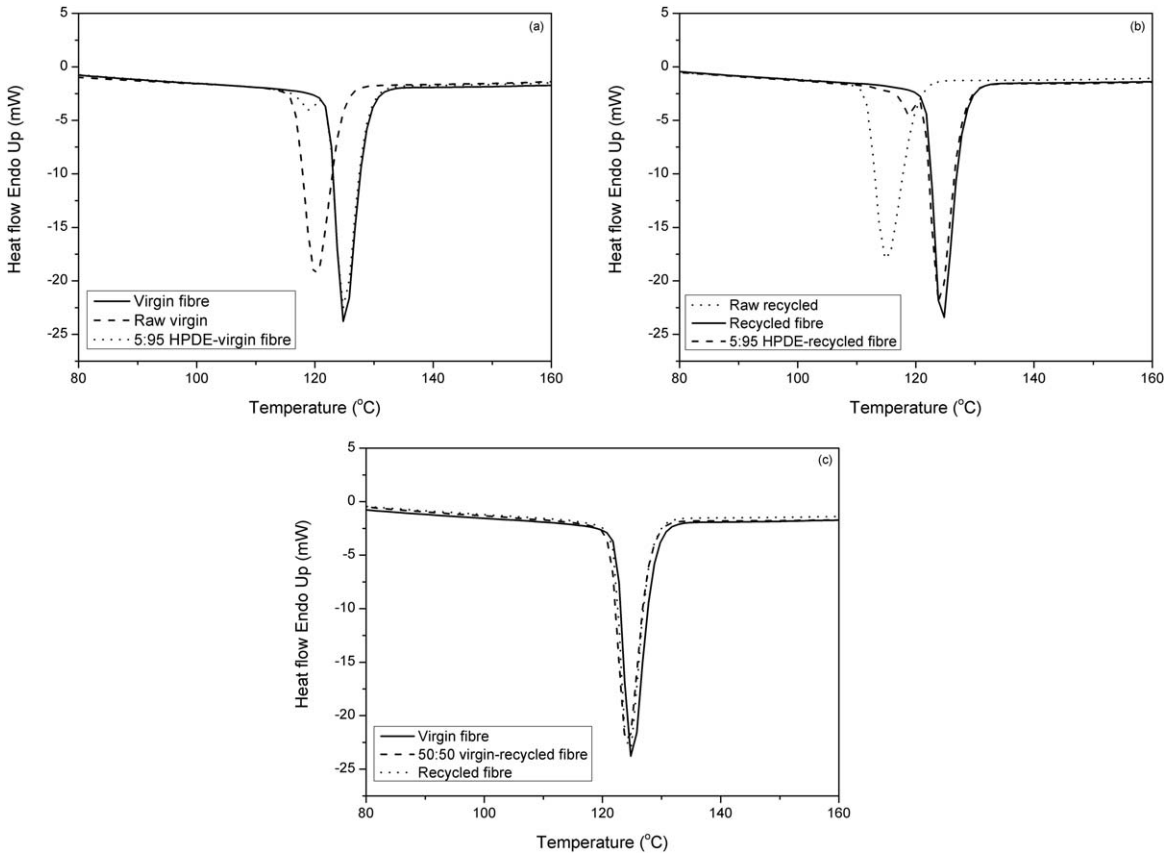

Figure 6. DSC heating curves of the PP fibers and their raw materials (cooling from 220 to 30°C).

As seen in Table III, the recycled PP fiber and virgin PP have similar ΔHs (105.4 J/g and 106.7 J/g, respectively) and similar crystallinity (50.9 and 51.5, respectively). However, as Figure 5(a,b) the recycled PP fiber has much higher ΔH on β-form crystals than the virgin PP fiber. The β-form crystals are much less stable than the α-form crystals.[42] Due to a large amount of β-form crystals, the recycled PP fiber showed lower tensile strength and Young modulus. Although the oriented α row-nuclei of the virgin PP fiber induced some β-crystals, the α-form crystals were still dominant and the ΔH of β-form crystals was very low in the virgin PP fiber. Therefore, the virgin PP fiber had a large amount of stable α-form crystals, thus showing higher tensile properties.

When 5% of HDPE was mixed with the virgin PP fiber as Figure 5(a), the ΔH of α-form crystals was decreased and the α-form crystallization was significantly affected by the heterogeneous structure between HDPE and virgin PP. Moreover, the HDPE offered nucleation sites for β-form crystals, thus improving rate of the β-form crystals. Therefore, the tensile strength and Young modulus of the virgin PP fiber was weakened by the HDPE. On the contrast, the 5% of HDPE restrained the formation of β-form crystals in the recycled PP fiber, more stable α-form crystals were produced by add the HDPE as Figure 5(b). The recycled PP normally has more molecular defects and lower purity due to the degradation in its service and processing history. The HDPE can act as a compatibilizer, which changes

Table III. Peak Temperatures of Melting and Heat of Fusion for the α- and β-Form Crystals (First Heating From 30 to 220°C)

PP compositions	T_m of α-form crystals (°C)	T_m of β-form crystals (°C)	Total ΔH (J/g)	Crystallinity (%)
Raw material of virgin PP	166.3		76.2	36.8
100% virgin PP fiber	170.3	152.8	106.7	51.5
5 : 95 HDPE-virgin PP fiber	169.8	153.3	100.5	48.6
Raw material of recycled PP	167. 8		85.9	41.5
100% recycled PP fiber	166.3	156.3	105.4	50.9
5 : 95 HDPE-recycled PP fiber	169.2	157.3	99.7	48.2
50 : 50 virgin-recycle fiber	169.8	154.3	104.8	50.6

Table IV. Peak Temperature of Crystallization and Heat of Fusion (Cooling From 220 to 30°C)

PP compositions	T_c (°C)	ΔH (J/g)
Raw material of virgin PP	119.8	88.4
100% virgin PP fiber	124.8	87.6
5 : 95 HDPE-virgin PP fiber	124.8	97.8
Raw material of recycled PP	114.8	87.9
100% recycled PP fiber	124.8	89.4
5 : 95 HDPE-recycled PP fiber	123.8	93.8
50 : 50 virgin-recycle fiber	123.8	87.3

rough phase structure of the molecular defects and some impurities, thus more stable α-form crystals were obtained.

When 50% of virgin PP was mixed with 50% of recycled PP as Figure 5(c), a double-melting endotherm is found on the α-form crystallization. One peak is located on 167°C, which is close to the T_m of α-crystals of recycled PP fiber; the other peak at 169.8°C, which is similar with the T_m of α-crystals of virgin PP fiber. Moreover, the ΔH of β-form crystals on 154.3°C is much lower than that of recycled PP fiber and slightly higher than that of virgin PP fiber. Therefore, the 50% of virgin PP not only retains high crystallinity and crystal structure, but effectively restrains the formation of β-form crystals in the recycled PP fiber. Finally, the 50 : 50 virgin-recycle fiber shows very high tensile strength and Young modulus as shown in Table II.

The samples were then held at 220°C for 5 min, and cooled from 220°C to 30°C at a scan rate of 10 K/min. As seen in Figure 6(a,b) and Table IV, the raw material of recycled PP has lower T_c (114.8°C) than the raw virgin PP (119.8°C), indicating that the raw recycled PP is easier to crystallize and can crystallize at a lower temperature. This is due to the lower molar mass and shorter molecular chains of recycled PP, which can be reflected by its lower MFI in Table I. According to Horvath *et al.*,[43] the shorter molecular chains are easier to be released from the strained or entangled macromolecules, thus the crystallization can be further developed by the rearrangement of these freed macromolecules segments. The heat of fusion of raw recycled PP is 87.9 J/g, which is lower than that of the raw virgin PP (88.4 J/g), indicating that the raw recycled PP released less thermal energy, formed fewer crystals and less perfect crystals than the raw virgin PP, because the raw recycled PP has more defective molecules and impurity.

As Table IV and Figure 6, after the melt spinning and hot drawing process, both the virgin and recycled PP fibers obtained much higher T_c (124.8°C) and more narrow crystalline peaks than their raw materials, indicating the hot drawing process highly oriented and aligned the crystal structures. When the temperature cooled down from the 220°C, the ordered molecular structure was more active at higher T_c and thus formed more perfect crystals than the raw materials, which leads to significantly improved mechanical properties of the fibers.

The heat of fusion of recycled PP fiber was improved to 89.4 J/g, because its short oriented molecular chains can be crystallized easily and quickly. However, the virgin PP fiber obtained lower heat of fusion (87.6 J/g) than its raw material. The oriented molecular chains of virgin PP fiber is more likely to form perfect crystals than its raw material, but it needs more time due to the long molecular chains. However, because of the same cooling rate in the DSC tests, the virgin PP fibers did not have enough time to form perfect crystals, thus obtained lower heat of fusion.[17] Moreover, the long molecular chains were easier to entangle and entwist together, thus deceased molecular order degree and crystallinity.[44]

When 5% of HDPE was mixed with the recycled and virgin PP fibers, their ΔHs were improved to 93.8 and 97.8 J/g, respectively, indicating the HDPE had heterogeneous nucleation effect on the PP crystallization. The crystallization of HDPE, which can be seen on the small peaks around 118.8°C in Figure 6(a,b), also contributed to the ΔHs. When 50% of the virgin PP was mixed with 50% of the recycled PP, the T_c and ΔH were slightly decreased probably due to compatible problems between the virgin and recycled PPs.

Thermal history of all the samples was eliminated through heating and cooling process, and then the samples were reheated from 30 to 220°C. As seen in Figure 7(a,b), the raw materials still have broad peaks, which are related to three-dimensional crystals known as spherulites and/or rows of lamellae.[39] Further, the raw material of the recycled PP has a broader peak than the raw material of the virgin PP, which indicates the crystals of recycled PP have broader size distribution. However, all the fibers show narrow peaks, because the highly chain-extended and the highly oriented crystalline blocks formed fibrils during the hot drawing process. The thermal history of highly extended and oriented molecular chain is hard to be fully eliminated in the first round of heating and cooling.[40] Small melting peaks from the HDPE can be found for the 5 : 95 HDPE-virgin PP fiber and 5 : 95 HDPE-recycled PP fiber. As Table V the T_ms of all the fibers are only about 165°C, which are much lower than the T_m of α-form crystals from the first heating in Table III, indicating that the hot drawing process highly extended and oriented crystalline blocks. Furthermore, the ΔHs of all the fibers in Table V are much lower than those in Table III, indicating that the hot drawing process significantly improved the crystallinity of the fibers.

Crystallinity by WAXS

Crystallinity of all the fibers and their raw materials was determined using WAXS measurements. In the Figure 8, the raw materials of virgin and recycled PP have four distinct diffraction peaks at at $2\theta = 14.2°$, 17°, 18.8°, and 21.4°/21.9°, associated with the (110), (040), (130), and (111)/(041) planes, respectively.[45] The peaks at $2\theta = 21.4°$ and 21.9° are the co-diffractions of β phase and α phase. The virgin and recycled PP fibers obtain five diffraction peaks at $2\theta = 14.2°$, 17°, 18.8°, 25.5°, and 28.4°. The α- and β- content of the PPs was calculated via the K-value of Turner Jones *et al.*:[46]

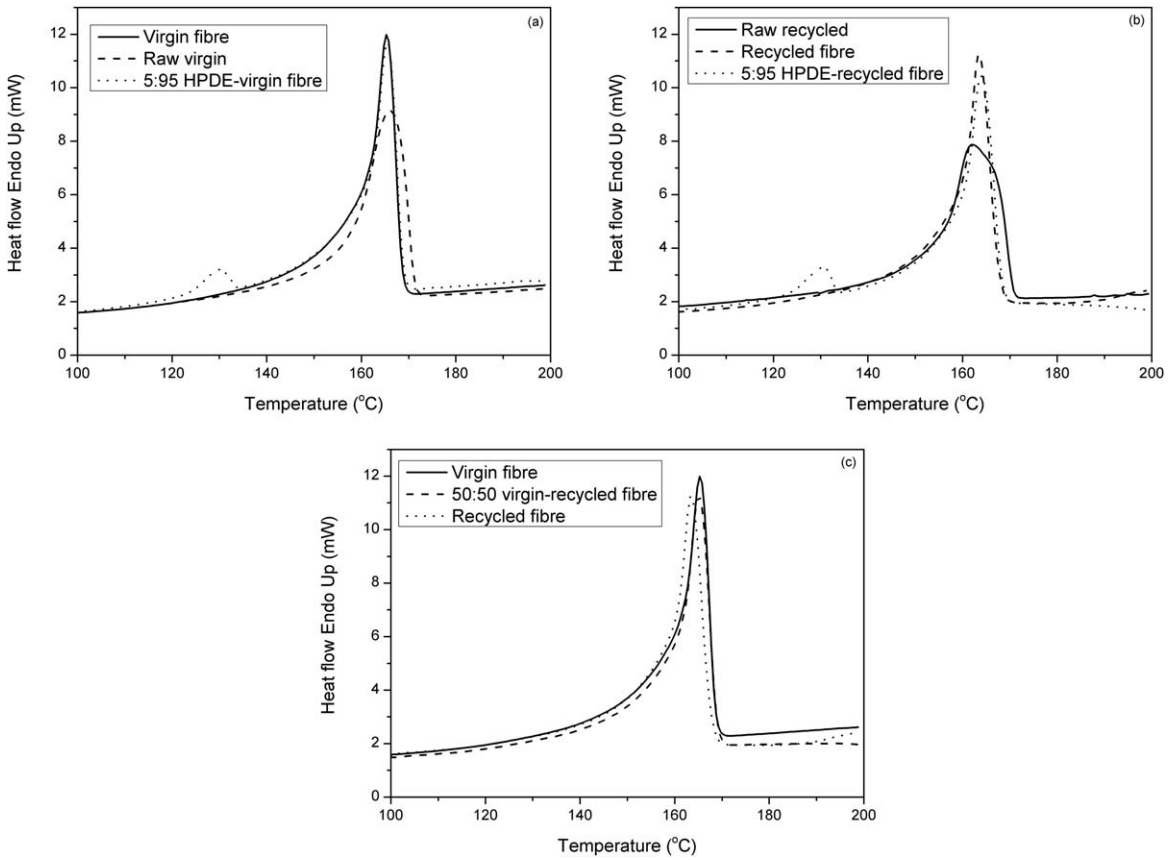

Figure 7. DSC heating curves of the PP fibers and their raw materials (second round of heating from 30 to 220°C).

$$K_\alpha = \frac{I_\alpha}{I_{\mathrm{HDPE}} + I_\alpha + I_\beta} \quad (3)$$

$$K_\beta = \frac{I_\beta}{I_{\mathrm{HDPE}} + I_\alpha + I_\beta} \quad (4)$$

Accordingly, $K_\alpha = 1$ and $K_\beta = 1$ for the fully α- and β-crystalline PP, respectively. The overall crystallinity (X_c) was determined by:

$$X_c = \frac{A_c}{A_c + A_a} \times 100 \quad (5)$$

where A_c and A_a are the areas under the crystalline peaks and amorphous halo, respectively.[30] The α-crystallinity is given by $K_\alpha X_c$, whereas for the β-crystallinity $K_\beta X_c$ holds. The crystallinity values derived from the WAXS measurements are summarized in Table VI.

As shown in Table VI the raw material of recycled PP has slightly higher crystallinity (51.2%) than the raw material of virgin PP (47.2%), because the raw material of recycled PP has lower molar mass, shorter molecular chains and more impurities. The lower molar mass and shorter molecular chains were

Table V. Peak Temperature of Melting and Heat of Fusion (Second Round of Heating from 30 to 220°C)

PP compositions	T_m (°C)	ΔH (J/g)
Raw material of virgin PP	164.8	83.2
100% virgin PP fiber	165.3	90.9
5 : 95 HDPE-virgin PP fiber	165.3	94.6
Raw material of recycled PP	161.8	84.3
100% recycled PP fiber	163.8	91.2
5 : 95 HDPE-recycled PP fiber	164.3	95.4
50 : 50 virgin-recycle fiber	165.3	92.8

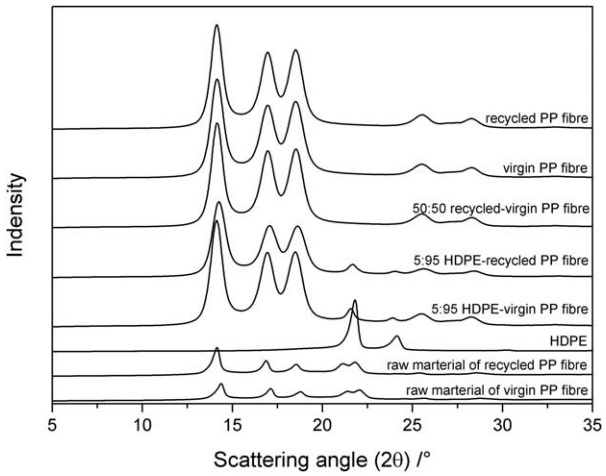

Figure 8. WAXS profiles of the PPs.

Table VI. Crystallinity of the Polypropylenes

Composition	Crystallinity (X_c)	$K_\alpha X_c$	$K_\beta X_c$
Raw material of virgin PP	0.472	0.40	0.077
100% virgin PP fiber	0.827	0.75	0.078
5 : 95 HDPE-virgin PP fiber	0.820	0.68	0.063
Raw material of recycled PP	0.512	0.43	0.078
100% recycled PP fiber	0.817	0.74	0.074
5 : 95 HDPE-recycled PP fiber	0.799	0.66	0.060
50 : 50 virgin-recycled PP fiber	0.819	0.75	0.071

easier to align and form into crystals, and the impurities greatly decreased the free enthalpy required for the formation of a critical nucleus, which further reduced the critical size of the nucleus and then led to the formation of heterogeneous nuclei.[47] However, the hot drawing process can considerably improve the crystallinity of the virgin and recycled PP fiber to 82.7% and 81.7%, respectively. The α-crystallinity (given by $K_\alpha X_c$) of the virgin and recycled PP fibers were significantly improved, while the β-crystallinity (given by $K_\beta X_c$) kept similar to their raw materials.

As shown in Figure 8, after the hot drawing process the virgin and recycled PP crystallize into the monoclinic α-form via diffractions at $2\theta = 14.2°$, 17°, and 18.8°, associated with the (110), (040), and (130) planes, respectively.[45] On these facets the diffraction peak positions have no change, but the intensities of the peaks increased drastically. The intensity of the diffraction peak reveals the crystallinity and orientation of materials. It indicates that the hot drawing process did not affect the α-form crystal type, but significantly improved the crystallization and orientation of the PP fibers. It was interesting to note that these three peaks overlapped to some extent, indicating that both crystal and mesomorphic phases co-existed in the fibers. The (111) and (041) doublet peaks moved to the off-axis and disappeared from the equator after the hot drawing process. On contrary, new peaks at $2\theta = 25.5°$, 28.4° are visible, indicating the generation of new β-form crystals.

When 5% of HDPE was added into the virgin and recycled PP fiber, both their crystallinity were slightly decreased due to the heterogeneous structure. The crystallization of HDPE restrained α- and β-crystallinity, as shown in Table VI. Therefore, the HDPE decreased the Young modulus of PP fibers, but increased the ductility of PP fibers as shown in Figure 3. However, when 50% of virgin PP was mixed with the recycled PP, the α-crystallinity kept as high as the virgin PP fiber, but the β-crystallinity was limited to lower rate of 6.9% (in Table VI). Therefore, 50 : 50 virgin-recycled PP fiber obtained the highest Young modulus in all the PP fibers.

CONCLUSIONS

This research explored the feasibility of using a melt spinning and hot drawing process to produce virgin and recycled PP fibers in the factory conditions, in an industrial scale. Virgin PP fibers of high tensile strength and Young modulus have been successfully produced by this method. However, the production of recycled PP fibers with sufficient mechanical properties is still a challenge due to the degradation that has taken place during its service life and heat processing stage. This study focused on improving tensile strength and Young modulus of recycled PP fibers by introducing 50% virgin PP or 5% HPDE during the manufacturing process. Finally, a relationship was established between the mechanical properties, crystallinity, crystal structure and orientation of the PP fibers. The following conclusions can be drawn:

1. The virgin PP fiber of high tensile strength (457 MPa) and high Young modulus (7526 MPa) was successfully produced by the melt spinning and hot drawing process under factory conditions. However, the recycled PP fiber produced by the same method showed significantly lower tensile strength (342 MPa), but comparable Young modulus (7115 MPa). Fibers made of virgin or recycled PP, modified with 5% HPDE showed higher ductility than the pure PP fibers. Fibers made from 50% virgin and 50% recycled PP showed similar tensile strength and higher Young modulus compared to the virgin PP fibers.
2. From the FTIR tests, the crystal molecular orientation was found in the recycled PP fiber. The orientated molecular structure offered the fiber high tensile strength and Young modulus.
3. After the melting spinning and hot drawing process, the melting enthalpy and crystallinity of the virgin and recycled PP fibers were increased dramatically. Both α-form and β-form crystals were found in the PP fibers. The virgin PP fiber had high rate of stable α-form crystals, thus obtaining high mechanical properties. However, the recycled PP fiber was found to have a large amount of less stable β-form crystals, so it had lower tensile properties. 5% of HDPE was found to decrease the α-form crystallization in the virgin PP fiber, while restrain the formation of β-form crystals in the recycled PP fiber. When 50% of virgin PP was mixed with 50% of recycled PP, the 50% of virgin PP not only retained high crystallinity and crystal structure, but effectively restrained the formation of β-form crystals in the recycled PP fiber.
4. From the WAXS measurements, the crystallinity of raw materials of virgin and recycled PP was measured as 47.2% and 51.2%, respectively. The melt spinning and hot drawing process significantly improved the crystallinity of virgin and recycled PP fibers to 82.7% and 81.7%. Therefore, the high tensile strength and Young modulus were obtained due to the significantly improved crystallinity.

REFERENCES

1. Daniel, J. I.; Gopalaratnamand, V. S.; Galinat, M. A. In ACI Committee 544, Report 544, 1R-96, American Concrete Institute, Detroit, USA, **2002**.
2. Zollo, R. F. *Cement Concrete Compos.* **1997**, *19*, 107.
3. Karahanand, O.; Atis, C. D. *Mater. Design* **2011**, *32*, 1044.
4. Takahashi, T.; Tsurunagaand, Y.; Kondo, T. *J. Appl. Polym. Sci.* **2013**, *130*, 981.
5. Sivakumarand, A.; Santhanam, M. *Cement Concrete Compos.* **2007**, *29*, 575.

6. Brandt, A. M. *Compos. Struct.* **2008**, *86*, 3.
7. Fraternali, F.; Ciancia, V.; Chechile, R.; Rizzano, G.; Feoand, L.; Incarnato, L. *Compos. Struct.* **2011**, *93*, 2368.
8. Smookand, J.; Pennings, A. J. *Polym. Bull.* **1983**, *9*, 75.
9. Vanhutten, P. F.; Koning, C. E.; Smookand, J.; Pennings, A. J. *Polym. Commun.* **1983**, *24*, 237.
10. Ochi, T.; Okuboand, S.; Fukui, K. *Cement Concrete Compos.* **2007**, *29*, 448.
11. Gregor-Svetecand, D.; Sluga, F. *J. Appl. Polym. Sci.* **2005**, *98*, 1.
12. Kim, J. H. J.; Park, C. G.; Lee, S. W.; Leeand, S. W.; Won, J. P. *Compos. Part B-Eng.* **2008**, *39*, 442.
13. Kim, S. B.; Yi, N. H.; Kim, H. Y.; Kimand, J. H. J.; Song, Y. C. *Cement Concrete Compos.* **2010**, *32*, 232.
14. Foti, D. *Construct. Build. Mater.* **2011**, *25*, 1906.
15. de Oliveiraand, L. A. P.; Castro-Gomes, J. P. *Construct. Build. Mater.* **2011**, *25*, 1712.
16. Wang, J.; Maoand, Q. C.; Chen, J. N. *J. Appl. Polym. Sci.* **2013**, *130*, 2176.
17. Zhang, B.; Chen, J. B.; Zhangand, X. L.; Shen, C. Y. *J. Appl. Polym. Sci.* **2011**, *120*, 3255.
18. Rangasamy, L.; Shimand, E.; Pourdeyhimi, B. *J. Appl. Polym. Sci.* **2011**, *121*, 410.
19. Sakurai, T.; Nozue, Y.; Kasahara, T.; Mizunuma, K.; Yamaguchi, N.; Tashiroand, K.; Amemiya, Y. *Polymer* **2005**, *46*, 8846.
20. Lupke, T.; Dunger, S.; Sanzeand, J.; Radusch, H. *Polymer* **2004**, *45*, 6861.
21. Tabatabaei, S. H.; Carreauand, P. J.; Aji, A. *Polymer* **2009**, *50*, 3981.
22. Zuo, F.; Keum, J. K.; Chen, X. M.; Hsiao, B. S.; Chen, H. Y.; Lai, S. Y.; Weversand, R.; Li, J. *Polymer* **2007**, *48*, 6867.
23. Choiand, D. M.; White, J. L. *Polym. Eng. Sci.* **2004**, *44*, 210.
24. Gregor-Svetec, D. *J. Appl. Polym. Sci.* **2006**, *100*, 1067.
25. Lyondellbasell, Available at: https://polymers.lyondellbasell.com/, accessed June, **2013**.
26. Martogg, Available at: http://www.martogg.com.au/www/home/, accessed June, **2013**.
27. Pttpm, Available at: http://www.pttpm.com/product_hdpe.aspx, accessed June, **2013**.
28. A. D3822, ASTM Int., United States (**2007**).
29. Parthasarthy, G.; Sevegneyand, M.; Kannan, R. M. *J. Polym. Sci. Part B-Polym. Phys.* **2002**, *40*, 2539.
30. Cerqueira, D. A.; Rodriguesand, G.; Assuncao, R. M. N. *Polym. Bull.* **2006**, *56*, 475.
31. Yeo, S. Y.; Leeand, H. J.; Jeong, S. H. *J. Mater. Sci.* **2003**, *38*, 2143.
32. da Costa, H. M.; Ramosand, V. D.; de Oliveira, M. G. *Polym. Test.* **2007**, *26*, 676.
33. Villain, F.; Coudaneand, J.; Vert, M. *Polym. Degrad. Stab.* **1995**, *49*, 393.
34. Hinsken, H.; Moss, S.; Pauquetand, J. R.; Zweifel, H. *Polym. Degrad. Stab.* **1991**, *34*, 279.
35. Bahlouli, N.; Pessey, D.; Ahziand, S.; Remond, Y. *J. De Phys. Iv* **2006**, *134*, 1319.
36. Li, J.; Li, H. L.; Meng, L. P.; Li, X. Y.; Chen, L.; Chen, W.; Zhou, W. M.; Qiand, Z. M.; Li, L. B. *Polymer* **2014**, *55*, 1103.
37. Gonzalez-Gonzalez, V. A.; Neira-Velazquezand, G.; Angulo-Sanchez, J. L. *Polym. Degrad. Stab.* **1998**, *60*, 33.
38. Huo, H.; Jiangand, S. C.; An, L. J. *Polymer* **2005**, *46*, 11112.
39. Somani, R. H.; Yang, L.; Zhuand, L.; Hsiao, B. S. *Polymer* **2005**, *46*, 8587.
40. Zhaoand, X. W.; Ye, L. *Mater. Sci. Eng. A-Struct. Mater. Prop. Microstruct. Process.* **2011**, *528*, 4585.
41. Elias, M. B.; Machadoand, R.; Canevarolo, S. V. *J. Therm. Anal. Calorim.* **2000**, *59*, 143.
42. Hirose, M.; Yamamotoand, T.; Naiki, M. *Comput. Theor. Polym. Sci.* **2000**, *10*, 345.
43. Horvath, Z.; Menyhard, A.; Doshev, P.; Gahleitner, M.; Tranninger, C.; Kheirandish, S.; Vargaand, J.; Pukanszky, B. *J. Appl. Polym. Sci.* **2013**, *130*, 3365.
44. Zhongand, C. F.; Mao, B. Q. *J. Appl. Polym. Sci.* **2009**, *114*, 2474.
45. Huang, Y. P.; Chen, G. M.; Yao, Z.; Liand, H. W.; Wu, Y. *Eur. Polym. J.* **2005**, *41*, 2753.
46. Chen, H. B.; Karger-Kocsis, J.; Wuand, J. S.; Varga, J. *Polymer* **2002**, *43*, 6505.
47. Aurrekoetxea, J.; Sarrionandia, M. A.; Urrutibeascoaand, I.; Maspoch, M. L. *J. Mater. Sci.* **2001**, *36*, 2607.